

Modulation of the Self-assembled Structure of Biomolecules: Coarse Grained Molecular Dynamics Simulation

Baohua Ji* and Yonggang Huang†

Abstract: The mechanisms governing the self-assembled structure of biomolecules (single chain and bundle of chains) are studied with an AB copolymer model via the coarse grained molecular dynamics simulations. Non-local hydrophobic interaction is found to play a critical role in the pattern formation of the assembled structure of polymer chains. We show that the polymer structure could be controlled by adjusting the balance between local (short range) and non-local (long range) hydrophobic interaction which are influenced by various factors such as the sequences, chain length, stiffness, confinement, and the topology of polymers. In addition, the competition between the intrachain hydrophobic interaction and interchain hydrophobic interaction determines the structural transition of the chain bundles. This work may provide important insights into the fundamental physics in the structure control and the self-assembly of biomolecules for various practical applications.

keyword: Biomolecules, Structure control, Self-assembly, Coarse grained modeling, Molecular dynamics simulation

1 Introduction

The structure and mechanics of polymers, especially biopolymers/biomolecules, are areas of strong interest due to their important roles and wide applications in life/medical sciences, various biotechnologies and materials engineering. For instance, the molecular structure of polymers is important to medical applications where the folded single chain polymer structures such as unimolecular micelles are of interest in drug delivery (1), and toroidal condensates of DNA represent a promising method of gene transfection for gene therapy (2). Nanoscale patterning of antigen and antibody on silicon

and polymer substrates can be used for immunological assay or protein chip (3). The self-assembled domains of protein molecules in biological materials guide the dynamics of mineral deposition, which is critical for the mechanical strength of biological materials (3-4). Currently, the mechanisms governing the structures of polymers are far from being fully understood.

Is it possible to predict the equilibrium structure and estimate the functions of a polymer chain from its sequence? How to design and control the structure and properties of a polymer? These questions present a considerable challenge for understanding the fundamental physics of folding and self-assembly of polymer chains. The composition and sequence of monomers in the backbone of biopolymers further adds the complexity of the above problems. For example, proteins have sequences that are designed by the process of evolution and contain up to 20 different monomer types, representing an extreme example of this complexity. As an initial attempt to understand the folding of biopolymers, researchers have focused on the collapse of a simple polymer in poor solvent (6-7). The early studies in this area were restricted to the collapse of a homopolymer chain (9-15), while more recent interest is on the more complex copolymers and semi-flexible copolymers with focus on the structure of biomolecules and nanoscale applications(1). The so-called HP model (hydrophobic-polar model) has been employed to study the "collapse-reorganization" kinetics in protein folding by Chan & Dill (16-17). Relationships between chain stiffness and sharpness of coil-globule transition have been studied by de Gennes (18). There are efforts to design sequences with controlled properties (e.g., rapid folding to native state) in a manner that mimics biological process (6-7). Possible roles of local hydrophobic-polar patterns and different forms of copolymer model interaction schemes in the folding and design/evolution of proteins have also been explored (19-20).

Instead of trying to reproduce the complex sequence for

* Department of Engineering Mechanics, Tsinghua University, Beijing 100084, P. R. China

† Department of Mechanical and Industrial Engineering, University of Illinois, Urbana, IL61801, USA

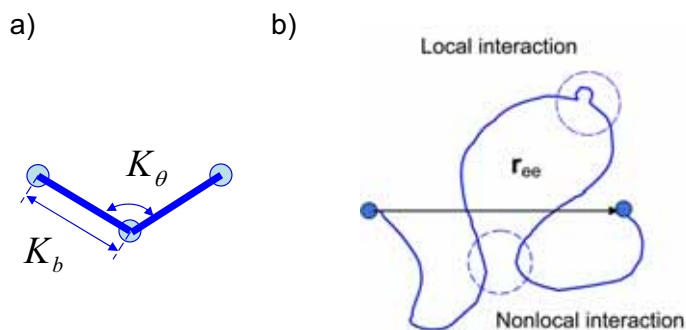


Figure 1 : (a) Schematic description of bond interaction including, bond connection and angle constraint, of monomers on a coarse grained “bead-spring” chain; the bond stiffness is represented by k_b , and angle stiffness is represented by k_θ . (b) Schematic illustration of non-bond interaction including, local and non-local interaction, on a polymer chain.

polymer molecules, we develop a simple model to understand the basic mechanisms of structure control of polymer chains. We may draw an analogy between design of model sequence for chain molecules to design of composite materials, which utilize the hardness of brittle constituent and toughness of soft constituent to control the mechanical properties of composite materials, and therefore introduce two competing mechanisms, namely hard vs. soft and brittle vs. tough. For designing model sequence for chain molecules, the basic idea may also be similar and simple, i.e., to introduce competing mechanisms in polymer sequence in order to control the microstructure/pattern of the structure in polymers. One way to achieve this is to design an inhomogeneous chain since introducing significant difference in the sequence of a polymer would help enrich the pattern of microstructures, which is consistent with the fact that protein molecules have complex hierarchical structures consisting of up to 20 different amino acids. The present work is aimed at finding the means of controlling the structure of polymer chains by introducing inhomogeneities in a polymer model that allows us to tune the strength of hydrophobic interaction which is the driving force for the folding and self-assembly of polymers. The simplest inhomogeneous chain model would be an AB copolymer consisting of only two types of monomers.

2 Simulation model and methods

2.1 Model

Biopolymers, such as DNA and protein molecules, are much more complex than AB copolymers and have up

to 20-letter sequences, side chains, and several types of interactions. However, the most essential distinction among monomeric units (amino acids) of protein molecules (12) is that some units are hydrophobic, while others are hydrophilic (21)(8). Therefore to a first order approximation the protein molecule can be modeled as an AB copolymer. Of course, such a simple model cannot describe and predict all features of protein molecules. Instead, it aims at revealing the essential physics of structure transition in polymer folding/self-assembly in order to find the mechanisms for controlling the structure of biopolymers at more macroscopic level than atomistic scale.

In the paper, we employ coarse-grained molecular dynamics method (22-23) to study the folding process and equilibrium properties of polymers. In comparison with full atom molecular dynamics simulation, the coarse grained approach enables the study of much larger system over much longer time. Our simulation model is illustrated in Figure 1a; coarse grained atoms (polymer monomers) are connected sequentially by linear springs (harmonic potential) to make bead-spring chains, and the stiffness of springs is k_b ; the angle of each bonded triplet is confined by a harmonic angle potential, and its stiffness is k_θ , giving bending rigidity to the chains. Even though there is no explicit solvent in the model, the effects of solvent are accounted for by additional non-bond interactions. For example, the hydrophilic behavior of monomers in solvent is effectively modeled by a shifted LJ potential (22-23),

$$U_P(r) = \begin{cases} 4\varepsilon_{LJ} \left[\left(\frac{\sigma}{r}\right)^{12} - \left(\frac{\sigma}{r}\right)^6 \right] + \varepsilon_{LJ} & r \leq r_{\min} = 2^{1/6}\sigma \\ 0 & r > r_{\min} = 2^{1/6}\sigma \end{cases} \quad (1)$$

where the subscript ‘‘P’’ indicates hydrophilic, and the potential has been cut off at its equilibrium position $2^{1/6}\sigma$ such that the hydrophilic monomers have no interactions beyond $2^{1/6}\sigma$ but strong repulsive interactions within $2^{1/6}\sigma$ in order to mimic the hydrophilic behaviors of monomers in a good solvent. The parameter σ represents the distance between two monomers at which their interaction energy vanishes, and σ sets the length scale in the model. The energy parameter ε_{IJ} governs the strength of interactions. The hydrophobic interaction between monomers is modeled by the LJ potential with a much larger cut off $R_c = 2.5\sigma$ in order to model the mutual attractive behaviors between monomers due to their hydrophobic effect in a poor solvent,

$$U_H(r) = \begin{cases} 4\varepsilon_{IJ} \left[\left(\frac{\sigma}{r}\right)^{12} - \left(\frac{\sigma}{r}\right)^6 - C(R_c) \right] & r \leq R_c \\ 0 & r > R_c \end{cases} \quad (2)$$

where the subscript ‘‘H’’ indicates hydrophobic, and $C(R_c) = (\sigma/R_c)^{12} - (\sigma/R_c)^6$. The interaction between hydrophobic and hydrophilic monomers is repulsion, modeled by Eq. (1). We use Lorentz-Berthelot mixing rules for parameters of the pair of hydrophobic and hydrophilic monomers in the simulation. These two modified LJ potentials capture the hydrophobic and hydrophilic effects, therefore can be used to model the process of folding and self-assembly of polymer chains. Since the dominant driving force for the folding/self-assembly of biomolecules is hydrophobic effect, in this work we focus on how to control the hydrophobic/hydrophilic interaction so that to control the equilibrium structures of the biomolecules. This study will not consider the electrostatic interactions.

The non-bond interactions between monomers, including the hydrophobic and hydrophilic interactions, are categorized into local and non-local interactions in this paper. As illustrated in Figure 1b, the local interaction refers to the interaction between two monomers which are close to each other in chain sequence and their distance typically ranges to several monomer sizes (short range interaction), while non-local interaction refers to two far

apart monomers in chain sequence which interact only after they come close due to the large deformation of the chain (long range interaction). Local interaction is short ranged, and sometimes could be easily blocked by the steric repulsion of neighboring monomers such that local interaction would not bring significant topological change to the chain conformation. On the contrary, it is normally easy for non-local interaction to bring significant topological change. For example, two far apart monomers of a chain adhere to each other due to strong hydrophobic interaction, which leads to the formation of a loop (Figure 1b). The non-local interaction is very important for a polymer chain to form complex pattern in the equilibrium conformation.

2.2 Methods

In the simulations, each monomer of the system moves according to the equation of motion,

$$m_i \ddot{r}_i = -\nabla V(\{r_i\}) - \Gamma \dot{r}_i + W_i(t) \quad (3)$$

where m_i is the mass and r_i the coordinates of the i th bead, $V(\{r_i\})$ the interaction potential, Γ is a (small) friction constant which couples the monomers weakly to a heat bath, while $W_i(t)$ is a Gaussian white-noise source. The strength of the noise is related to Γ via the fluctuation dissipation theorem. The equations were integrated with a time step $\Delta t = 0.005\tau$, where $\tau = \sigma(m/\varepsilon)^{1/2}$ is the standard time unit for a Lennard-Jones system. In this paper, we will present most of our results in reduced units in which $\sigma = m = 1$, ε_{IJ} in unit of $k_B T$, where k_B is Boltzmann constant. We set $T = 1.0$ and $\Gamma = 0.5\tau^{-1}$. The introduction of a weak coupling to a thermal bath is very important not only to keep the temperature at the preset value but also to keep the system stable over the course of the simulation. We made runs up to $2 \times 10^7 \Delta t$ after the chains are equilibrated from the initial configuration. Most systems reached equilibrium within a nondimensional time of at most a few ten thousand for short and intermediate chains. The simulations were continued until the nondimensional time 50000 for long chains ($N > 300$), and then extended by another 50000 time units for data accumulation.

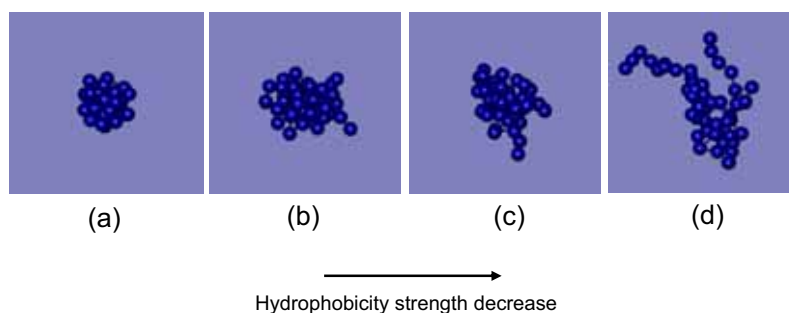


Figure 2 : The snapshots of the structural evolution of homogeneous chains as the strength of hydrophobicity of monomers decreases ($N=50$).

3 Results and discussions

3.1 Structures of single chain

We begin with the study of folding process of a single homogeneous chain ($N=50$, N denotes the number of monomers in the chain). Its comparison with that for inhomogeneous chains will reveal the unique characteristics of the latter. All simulations start from a straight initial conformation where the monomers are aligned sequentially along a straight line. Figure 2 shows the snapshots of the evolution of the collapsed configuration of the chain as the strength of hydrophobicity [ϵ_{IJ} in equation (2)] decreases. It is note that there is no distinct microstructure in the final conformation of homogeneous chain no matter how the strength of hydrophobic interaction changes. This confirms our hypothesis that homogeneousness would not favor the creation of microstructures in the self-assembled polymer structure. Inhomogeneous should play a critical role in the microstructure and pattern formation in polymer systems. Different inhomogeneous in the chain system may include hydrophobic vs. hydrophilic, long vs. short, stiff vs. flexible, and slow vs. fast in dynamics.

We now study the simplest inhomogeneous chain, an AB copolymer, which has two types of blocks, A and B. Block A consists of n hydrophobic monomers and block B consists of the same number of hydrophilic monomers, where we choose $\epsilon_{IJ}^H = 4$ for the hydrophobic, and $\epsilon_{IJ}^P = 1$ for the hydrophilic. These two blocks alternate along the chain in the chain sequence. Figure 3a illustrates the sequence and the periodic unit of the copolymer. For m periodic units, there are $N=2mn$ monomers which give the chain length of the copolymer. We first study the equilibrium conformation of a flexible AB copolymer which has a small constant $k_\theta = 1$ for

both blocks A and B in the reduced dimension. The inhomogeneous chain exhibits drastically different behavior (Figure 3b) in comparison with its counterpart for homogeneous chains shown in Figure 2. Microstructures are formed in the equilibrium conformation of chains at various lengths as shown in Figure 3b: hydrophobic monomers collapse to hydrophobic cores, and the hydrophilic monomers wrap the hydrophobic cores and separate them from the other part of the chain by the “flower leaves” structures, forming spherical micelle-like structures linked by single hydrophilic chain segment. The whole chain looks like a beautiful pearl necklace. It should be pointed out that, although the micelle-like necklace structure is created for the AB copolymer with hydrophobic and hydrophilic blocks, its geometric structure is still a generally linear structure without long range network of branching and loops.

The mechanism that soft chains prefer to create linear micelle-like necklace structures is related to the local hydrophobic interaction. Since the local dynamic is faster than the global dynamic of chains, the local hydrophobic effect controls the folding process of soft chains. Specifically, the (local, fast formed) micelle-like structures nucleate much earlier than the (non-local, slowly formed) loop formation such that the non-local interaction has no chance to create the loop after the micelle-like structures mature (hydrophobic cores are wrapped by the hydrophilic leaves, losing hydrophobicity effectively). In the course of micelle-like structure formation, hydrophilic segments bend to allow the hydrophobic monomers to congregate. Therefore, increasing the stiffness of hydrophilic segments can effectively block the local interaction by a higher energy barrier to the congregation of neighboring hydrophobic monomers to gain time for the dynamics of the non-local interaction. In compar-

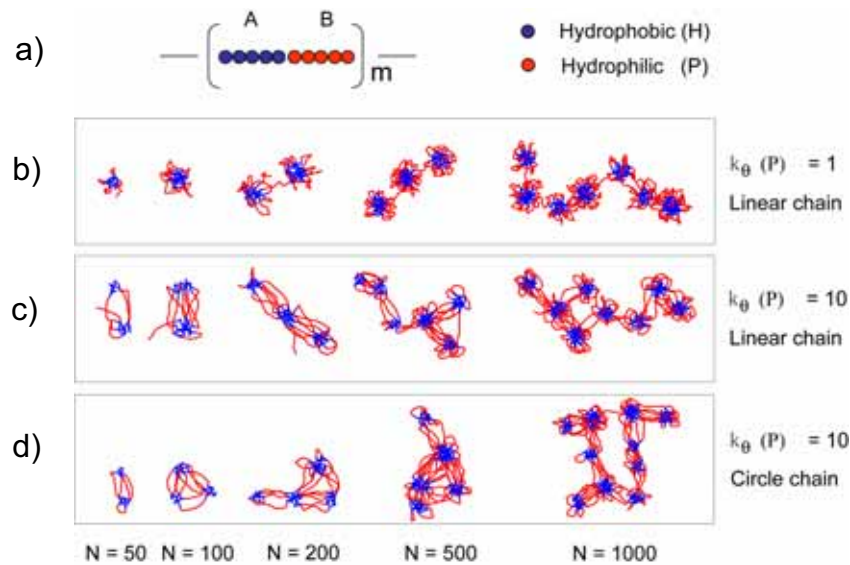


Figure 3 : The snapshots of the self-assembled structures of inhomogeneous chains. (a) Schematic illustration of the chain sequence and the periodic unit of AB copolymers. The block size of A/B block n equals 5. (b) The self-assembled structures of linear flexible AB copolymer chains at various chain lengths. (c) Structures of linear stiff AB copolymer chains at various chain lengths. (d) Structures of closed circle stiff AB copolymer chains at various chain lengths.

ison, the radius of curvature of the chain caused by the deformation due to non-local interaction is much larger (longer range) than that due to local interaction such that the hydrophilic segments need not bend as severely as for local interaction when two far apart monomers congregate and contact to have non-local interaction (see Figure 1b). Therefore, increasing the chain stiffness will not block the non-local interaction severely. The non-local interaction between two hydrophobic monomers helps to create branch, loop and other complex patterns. We take a much larger angle constant $k_\theta = 10$ for the B block in order to increase the bending stiffness of hydrophilic segments. Figure 3c shows that the stiffened chains self-fold into more complex pattern at various chain lengths in contrast to those of flexible AB copolymer. In addition, the end effect of chains is found to be an important mechanism to trigger non-local interaction: big conformation change always starts from the two ends, and then propagates towards the center of the chain. However, the end effect becomes weak if the chain is very long, and other mechanisms are needed to trigger the non-local interaction.

One possible way to trigger more non-local hydrophobic interaction is to make chain conformation more favorable for non-local interaction. For example, large curvature of

chain increases the probability of non-local interaction and enhances the formation of complex pattern structures. A good candidate for this purpose might be the circle conformation where the two ends of the chain are connected by harmonic bond in comparison with the linear chain with free ends. The curvature reduces the distance between monomers that are initially far apart along the chain in sequence, and promotes monomers to have non-local interactions. The closed chains with circular conformation evolve into more complex pattern than the linear chain, as shown in Figure 3d. For example, the circle chain with $N=100$ forms a triangle pattern that is stabilized by the stiff hydrophilic segments. As the chain becomes longer, complex long range branches and network still form, in comparison with those of the linear chains in Figures 3b and c, implying that the topology of chain plays very effective roles.

Figure 4 shows the evolution of the radius of gyration and total energy during the folding process of the linear flexible copolymer chain (chain #1), linear stiff copolymer chain (chain #2), and the circular stiff copolymer chain (chain #3, two ends are connected), respectively, at $N=500$. It is seen that the dynamics of chain #2 is much slower than that of chain #1 because the stiffer hydrophilic segment of chain #2 puts a higher elastic en-

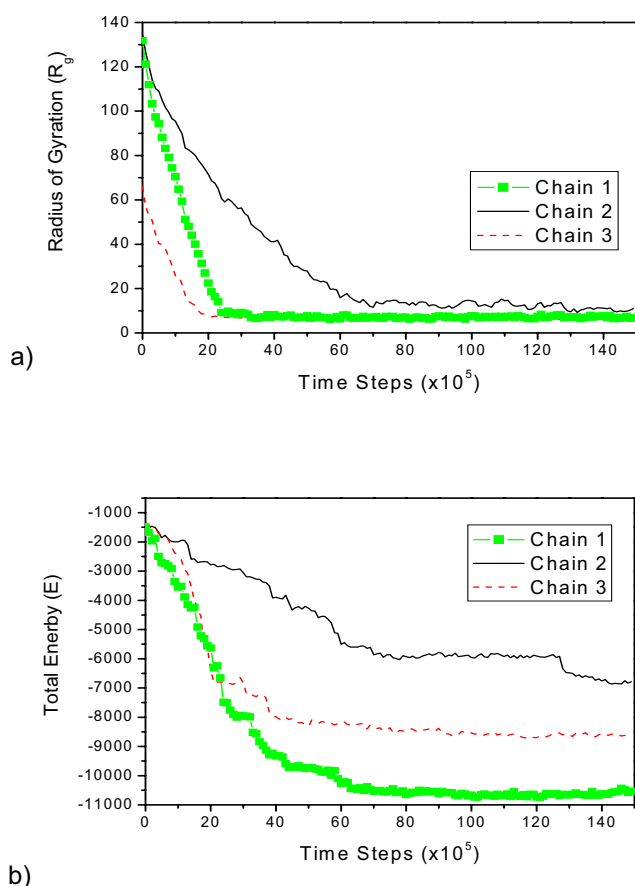


Figure 4 : Evolution of the radius of gyration (a) and the total energy (b) of AB copolymer chains during the folding process for linear flexible chain (#1), linear stiff chain (#2) and circle stiff chain (#3), respectively, at $N=500$. It is noticed that, after the radius of gyration reaches to the equilibrium size at specific time (at about 20×10^5 time steps for linear flexible chain and circle stiff chain, and at about 70×10^5 time steps for linear stiff chain), the decrease of total energy can still happen afterwards.

ergy barrier to both local and non-local interactions and thus slows down the dynamics of the chain. For all three chains, the total energy fluctuates and reaches one or several plateaus at a metastable state after rapid decrease at the early stage of folding process. It takes the chains a long time at the plateau to search for the pathway to the next lower energy states (as 1st order transformation) (24)(25)(26). It is interesting to observe that the total energy of chains continues to decrease after the radius of gyration of chains reaches the equilibrium value, which implies the internal microstructure re-organization of the

chain conformation at a fixed global size.

In contrast to the previous controlling mechanisms of enhancing the non-local interaction, the constraint can also be introduced to control the self-assembled structure of polymers. A natural choice of constraint is a cylindrical confinement which mimics a nanopore or nanochannel. If the radius of confinement is smaller than the radius of gyration of polymer, it will confine the dynamics of the chain by suppressing its non-local hydrophobic interaction. Figure 5a shows a cylindrical confinement with radius being about 5 times of the bond length of the polymer, where a hydrophobic coil (segment A) can have non-local interaction with its second hydrophobic neighbor (NB C) through hinge motion with respect to its first hydrophobic neighbor (NB B), but it will be difficult for A to have non-local interaction with its third and fourth neighbors to form loop due to the confinement of the cylinder wall (see Figure 5b). Therefore, the final configuration of a stiff linear copolymer ($N=500$) is globally a linear structure without loop and branching, as the non-local interactions except that through hinge motions are suppressed by the confinement, and the local hydrophobic interaction is confined by the stiff hydrophilic segment as well. Hinge motion of the hydrophobic coils dominates the dynamics of non-local interaction, as we can see that hydrophobic cores are normally connected by multiple hydrophilic segments caused by hinge motions. When we halve the radius of the confinement, the hinge motions are severely confined so that the energy barrier is even larger than that for local interaction, therefore the pearl-necklace structure is more favored at this time as show in Figure 5c. Compared with Figure 3b of the soft linear chain (for case of $N=500$), the confined linear stiff chain has more but smaller pearl structures in the final conformation (5 pearls vs. 3 pearls) as it is more difficult for the pearl to aggregate to be larger by bending more stiff hydrophilic segments.

3.2 Structures of chain bundles

The self-assembly of a bundle of chains should be more complex, and the structure should be much different from that of single chain. Bundle of chains can introduce more non-local interactions since monomers from different chains may interact. An example of chain bundles is collagen fibril or fiber in bone materials. The dynamics of chains is confined by their neighbors in the bundle such that the non-local interaction between

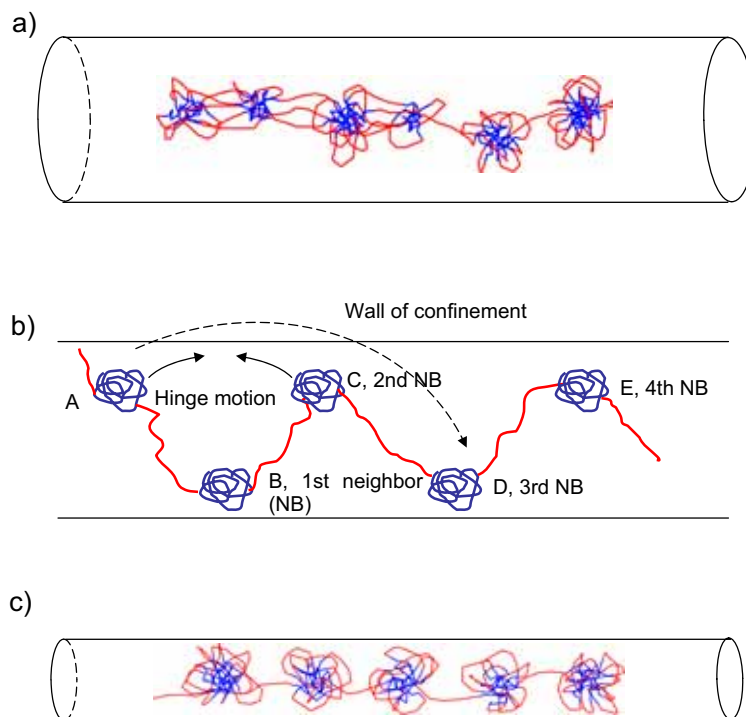


Figure 5 : The self-assembled structure of a single chain in a cylindrical confinement. a) The radius of the cylinder is 5 times of the bond length of the chain, at which the hinge motion of the hydrophobic coils of chain dominates the non-local hydrophobic interaction; b) Schematic illustration of the hinge motion of a hydrophobic coil A with its second neighbor B. It will be difficult for coil A to have non-local interaction with its third and fourth neighbors (D and E) to form loop due to the confinement of the cylinder wall, e.g. the path of the dash line for A to contact with D is constrained; c) The radius of the cylinder is halved (2.5 times of the bond length), at which all the non-local hydrophobic interaction are forbidden, so that a pearl-necklace structure is formed.

monomers can be controlled by the alignment and distance between chains. In the simulation, the initial structures of chains in bundle are straight parallel lines and the chain distance defines the density of the bundle. The simulation model of chain bundle has been set up as following: each chain is protruded in Z direction from a lattice node of a quadrangular lattice on XY plane, and the distance and alignment between the chains can be well controlled by adjusting the lattice structure. We take the sequence of short single chain with two periodic units (AAAAABBBBBAAAAABBBBB) in the simulations of the self-assembly of chain bundle, i.e., $m=2$ and $n=5$, which gives $N = 2nm = 20$ (see Figure 6a). We find that the chain bundles exhibit interesting pattern in their final conformation, as shown in Figures 6b to 6g, where the structure of chain bundle evolves with its size, the number of chains M . For a small bundle with small number of chains ($M=10$, Figure 6b), a micelle-like structure forms with one hydrophobic core, where

the constraint of the bundle on the chains is weak and the self-folding of individual chain plays dominant role; as the number of the chain increases, two and four domains of hydrophobic cores form for $M=50$ and $M=100$ (Figure 6c & d), respectively, where the interchain non-local interaction between chains in the bundles is still weak; for $M=200$, the interchain interaction takes effective roles in the self-assembly of the bundle, and a worm like structure forms due to strong confinement of the bundle on individual chain (Figure 6e); further increasing the chain number $M=300$ (Figure 6f), the bundle forms a double-layered micelle-like structure (more condense) due to the enhanced constraint, and it is noted that the structure is more complex than the micelle structure self-assembled by amphiphilic single molecules (25). This difference is because the polymer chain with two periodic units can be considered as two amphiphilic single molecules being connected sequentially, which double the non-local interaction sites for neighboring chains, therefore allow the

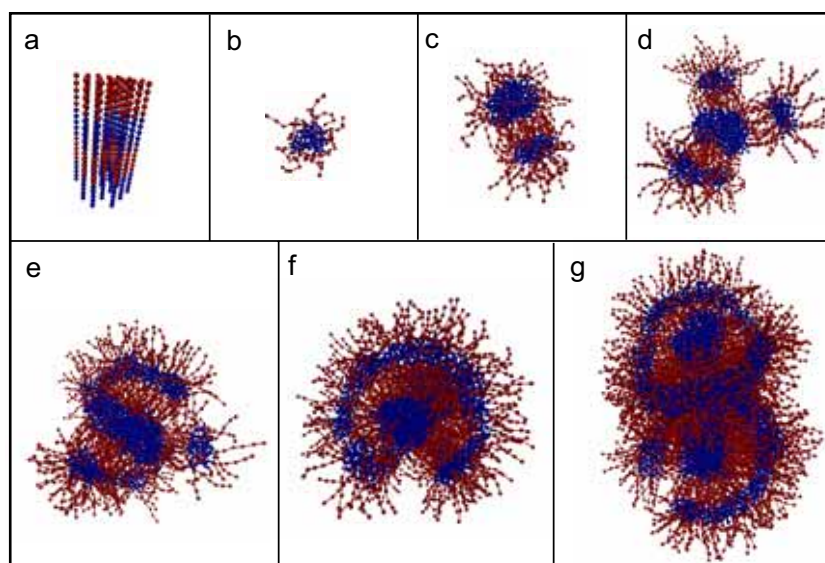


Figure 6 : Self-assembly of bundles of polymer chains. The size of the bundle (or M , the number of chains in bundle) can influence the final structure of the bundle. a) The initial conformation of a chain bundle; b) $M=10$, a micelle-like structure forms, where the self-folding of single chain plays dominant roles; c) $M=50$, two domains form; d) $M=100$, the interchain interaction is still weak in the bundle, the bundle splits into four domains; e) Worm like structure forms due to somewhat stronger constraint and interchain interaction in the bundle for $M=200$; f) When the chain number is increased to $M=300$, the bundle forms a double layered micelle-like structure due to enhanced constraint and interchain interaction; g) Twin micelle structure forms at $M=600$ because of the even stronger confinement of the bundle, where the global assembly of the bundle dominates the self-assembly of the bundle.

bundle to form more complex pattern. Figure 6g shows twin micelle-like structure forms at $M=600$ because of even stronger confinement of bundle, where the global assembly of the bundle overwhelmingly dominates the dynamic of the system and the self-assembly process of individual chain has been severely suppressed.

The underneath mechanism for the structural transition of chain bundles shown in Figure 6 is the competition between the self-assembly of single chain (dynamics of individual chain through intrachain interaction) and the global self-assembly of the bundles (dynamics of the whole system through interchain interaction). Because of the confinement of the bundles, the dynamics of a single chain in the bundle is interfered by its neighboring chains, e.g., as soon as the chain is interacted with its neighbors and then contact with them, it can not fold as easily as at its free state, and therefore its self-assembly process is interrupted and slowed. This further provides more opportunities for the interchain non-local interaction between chains to take place for global assembly. The more chains the bundle has, the stronger confinement it can provide. Figure 7 shows this mechanism

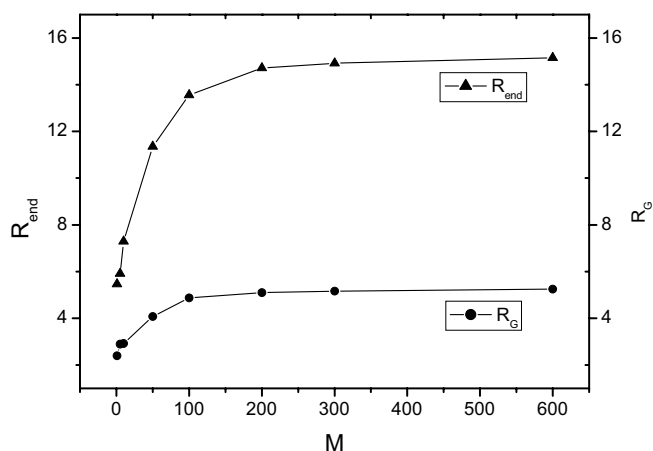


Figure 7 : The evolution of the average end to end distance R_{end} and radius of gyration R_G of chain bundles as the number of chains M (the size of bundle) increases.

through the evolution of the average (ensemble average) end to end distance (R_{end}) and radius of gyration (R_G) of single chain. When the number of the chains is small, the confinement to individual single chain is weak, there-

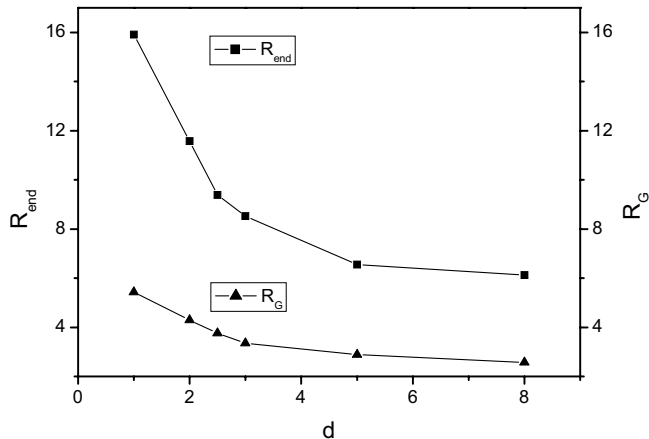


Figure 8 : The evolution of end to end distance R_{end} and radius of gyration R_G of chain bundles as the chain distance d (in unit of $2^{1/6}\sigma$) increases.

fore the chain can easily fold to itself native state, so that its end to end distance and the radius of gyration reduce quickly and at the same time it loses its hydrophobicity (hydrophobic core embedded by hydrophilic segments) in a short time before it could contact with its neighbors, therefore the end to end distance and the radius of gyration of the final state of each single chain is small. When the number of chains becomes larger, the confinement from the bundle becomes stronger, i.e. each chain has more contact with its neighbors and then should deform together with the neighbors, therefore its self-folding has been strongly confined and thus the end to end distance and the radius of gyration of its final state do not reduce so much. When the chain number is increased up to 200 or larger, R_{end} and R_G approaches to their limiting value, respectively, which depend on the chain distance in the bundle.

To check the effect of the chain distance on the structure of chain bundle, we simulate the self-assembly of chain bundle with various chain distance. We monitor the average end to end distance and the radius of gyration of individual chain as the chain distance is changed which resembles the variation of the concentration of polymer in solvent. The simulation shows that as the chain distance increases, the confinement of chain bundles on individual chain becomes weak, which encourages the self-folding of individual chain, so that the single chain has enough time to fold to its individual native state and becomes more hydrophilic globally (hydrophobic core embedded by hydrophilic segments), further weakening the inter-

chain interaction. Figure 8 shows the evolution of R_{end} and R_G with the chain distance increasing. We note that as the chain distance approaches a limiting value, the interchain interaction becomes so weak that the dynamics of the whole system mainly depends on the dynamics of individual chain. Figure 9a-d shows the structure transition of a bundle with 100 chains as the chain distance is continuously increased. We find that the conformation of chain bundle largely depends on the initial conformation of the single chain when the distance is very small where the dynamics of the individual chain is severely confined and blocked, and the global structure of bundle just resembles the initial conformation of individual chain as shown in Figure 9a. At an intermediate chain distance the bundle forms a complex network shown in Figure 9c. When the chain distance is very large, the dynamics of single chain dominates the final structure of the bundle which forms separating polymer coils dispersed in the system as shown in Figure 9d. Huo (Personal communications) saw similar structural transition of degenerated silk protein by changing the protein concentration in his experiments.

4 Conclusions

The motivation of this study is to find possible approaches to control the dynamics and structure of biomolecules. Through the coarse grained molecular dynamics simulations we show that non-local hydrophobic interaction is crucial for structural transition and pattern formation of the self-assembled structure of polymer chains. The competition between local and non-local interactions might be used to control the process of self-assembly and folding of polymers. It is shown that the non-local interaction can be tuned with the stiffness, length, topology and confinement of chains. The high local stiffness of hydrophilic segment can severely suppress the local interaction and thus promote the non-local hydrophobic interaction. The end effect of polymer chains can enhance the non-local hydrophobic interaction, particularly for short chains. The topology of chain provides an effective means of introducing a large amount of non-local interaction. Furthermore, we demonstrated that the competition between the intrachain hydrophobic interaction and interchain hydrophobic interaction takes important roles for structure transition of chain bundles. The competition can be controlled by modulating the size of the bundle (the number of the

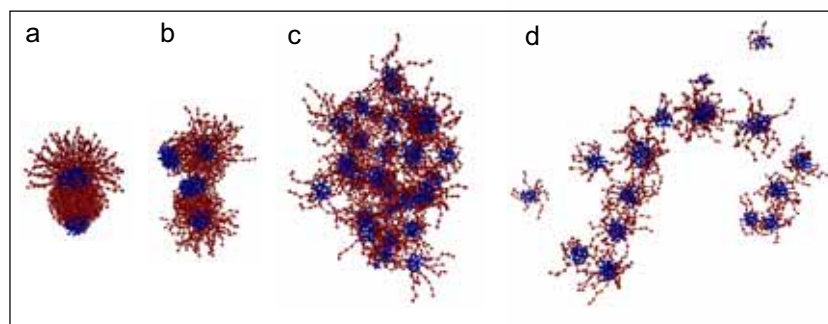


Figure 9 : The snapshots of the self-assembled structure of bundles as the chain distance increases. a) When the distance is very small ($d = 1$), the global assembly dominates the dynamics of the bundle due to strong interaction between chains; b) The self-folding of single chain takes roles in the structural transition of bundle, and multiple domains forms at $d = 2$; c) The interchain interaction become weaker, a network of multiple hydrophobic cores forms at $d = 2.5$; d) When the distance become very large ($d = 4$), interchain interaction takes minute roles and the self-assembly of individual chain dominates.

chains in the bundle), and the distance between the chains in the bundle. These findings might allow us to understand some important mechanisms of nature controlling the complex 3-D structure of proteins as well as those of other functional biomolecules in cell and extracellular matrix (ECM), namely the complex sequence with abundant amino acids or other monomers gives nature a lot of flexibilities to choose different competing mechanisms in order to design and control the local and non-local hydrophobicity of chains, as well as the intrachain interaction and interchain interaction, which consequently determine the 3-D structure of biomolecules.

Acknowledgement: This work is supported by the National Natural Science Foundation of China through Grant No. 10442002, 10502031, 10628205, 10121202, Tsinghua Basic Research Foundation, and National Basic Research Program of China through Grant No. 2004CB619304, and SRF for ROCS, SEM. BJ thanks for the helpful discussion with Prof. Huajian Gao at Max-Planck Institute for Metal Research and now at Brown University.

References

1. Liu, H. B., Farrell, S., Uhrich, K. (2000) Drug release characteristics of unimolecular polymeric micelles, *Journal of Controlled Release*, **68**, 167-174.
2. Blessing, T., Remy, J. S., Behr, J. P. (1998) Monomolecular collapse of plasmid DNA into stable virus-like particles, *Proc. Natl. Acad. Sci. USA*, **95**, 1427-1431.
3. Laine, R. M., Choi, J. W., Lee, I. (2001) Organic-inorganic nanocomposites with completely defined interfacial interactions, *Advanced Materials*, **13**, 800-803.
4. Gao, H., Ji, B., Jager, I. L., Arzt, E., Fratzl, P. (2003) Materials become insensitive to flaws at nanoscale: Lessons from nature, *Proc. Natl. Acad. Sci. USA*, **100**, 5597-5600.
5. Ji, B., Gao, H. (2004) Mechanical properties of nanostructure of biological materials, *J. Mech. Phys. Solids*, **52**, 1963-1990.
6. Yue, K., Dill, K. A. (1992) Inverse protein folding problem: designing polymer sequences, *Proc Natl Acad Sci U S A.*, **89**, 4163-4167.
7. Shakhnovich, E. I., Gutin, A. M. (1993) Engineering of stable and fast-folding sequences of model proteins, *Proc. Natl. Acad. Sci. USA*, **90**, 7195-7199.
8. Khokhlov, A. R., Khalatur, P. G. (1999) Conformation-dependent sequence design (engineering) of AB copolymers, *Physical Review Letters*, **82**, 3456-3459.
9. Sanchez, I. C. (1979) Phase Transition Behavior of the Isolated Polymer Chain, *Macromolecules*, **12**, 980-987.

10. Williams, C., Brochard, F., Frisch, H. L. (1981) Polymer collapse, *Ann. Rev. Phys. Chem.*, **32**, 433-451.
11. Ostrovsky, B., Baryam, Y. (1994) Irreversible Polymer Collapse In 2 And 3 Dimensions, *Europhysics Letters*, **25**, 409-414.
12. Timoshenko, E. G., Dawson, K. A. (1995) Equilibrium properties of polymers from the Langevin equation: Gaussian self-consistent approach, *Phys. Rev. E*, **51**, 492-498.
13. Timoshenko, E. G., Kuznetsov, Y. A., Dawson, K. A. (1995) Kinetics At The Collapse Transition Gaussian Self-Consistent Approach, *Journal of Chemical Physics*, **102**, 1816-1823.
14. Klushin, L. I. (1998) Kinetics of a homopolymer collapse: Beyond the Rouse-Zimm scaling, *Journal of Chemical Physics*, **108**, 7917-7920.
15. Halperin, A., Goldbart, P. M. (2000) Early stages of homopolymer collapse, *Physical Review E*, **61**, 565-573.
16. Chan, H. S., Dill, K. A. (1993) Energy landscapes and the collapse dynamics of homopolymers, *Journal of Chemical Physics*, **99**, 2116-2127.
17. Chan, H. S., Dill, K. A. (1994) Transition-States And Folding Dynamics Of Proteins And Heteropolymers, *Journal of Chemical Physics*, **100**, 9238-9257.
18. de Gennes, P.-G. (1975) *Le Journal de Physique-Lettres*, **36**, L55.
19. Cui, Y., Wong, W. H., Bornberg-Bauer, E., Chan, H. S. (2002) Recombinatoric exploration of novel folded structures: A heteropolymer-based model of protein evolutionary landscapes, *Proc. Natl. Acad. Sci. USA*, **99**, 809-814.
20. Wroe, R., Bornberg-Bauer, E., Chan, H. S. (2005) Comparing folding codes in simple heteropolymer models of protein evolutionary landscape: Robustness of the superfunnel paradigm, *Biophysical Journal*, **88**, 118-131.
21. Grosberg, A. Y. (1997) *Phys.-Usp.*, **40**, 109-113.
22. Micka, U., Holm, C., Kremer, K. (1999) Strongly charged, flexible polyelectrolytes in poor solvents: Molecular dynamics simulations, *Langmuir*, **15**, 4033-4044.
23. Limbach, H. J., Holm, C. (2001) End effects of strongly charged polyelectrolytes: A molecular dynamics study, *Journal of Chemical Physics*, **114**, 9674-9682; EsPResSo, <http://www.espresso.mpg.de/>.
24. Timoshenko, E. G., Kuznetsov, Y. A., Dawson, K. A. (1996) Gaussian self-consistent method for the kinetics of heteropolymers: A direction in studying the protein folding problem, *Phys. Rev. E*, **53**, 3886-3899.
25. Huang, K. (2001) Lectures on statistical physics and protein structure., Massachusetts Institute of Technology. Cambridge, MA USA, and Zhou Pei-Yuan Center for Applied Mathematics, Tsinghua University, Beijing, China.
26. Cooke, I. R., Williams, D. R. M. (2003) Collapse dynamics of block copolymers in selective solvents: Micelle formation and the effect of chain sequence, *Macromolecules*, **36**, 2149-2157.

